Numerical study of lattice Boltzmann methods for a convection–diffusion equation coupled with Navier–Stokes equations

2011 J. Phys. A: Math. Theor. 44 055001

(http://iopscience.iop.org/1751-8121/44/5/055001)

IOP PUBLISHING JOURNAL OF PHYSICS A: MATHEMATICAL AND THEORETICAL

J. Phys. A: Math. Theor. **44** (2011) 055001 (18pp) doi:10.1088/1751-8113/44/5/055001

Numerical study of lattice Boltzmann methods for a convection–diffusion equation coupled with Navier–Stokes equations

H-B Huang[1], **X-Y Lu**[1] **and M C Sukop**[2]

[1] Department of Modern Mechanics, University of Science and Technology of China, Hefei 230026, People's Republic of China
[2] Department of Earth and Environment, Florida International University, FL, USA

E-mail: huanghb@ustc.edu.cn

Received 15 June 2010, in final form 7 December 2010
Published 4 January 2011
Online at stacks.iop.org/JPhysA/44/055001

Abstract

Numerous lattice Boltzmann (LB) methods have been proposed for solution of the convection–diffusion equations (CDE). For the 2D problem, D2Q9, D2Q5 or D2Q4 velocity models are usually used. When LB convection–diffusion models are used to solve a CDE coupled with Navier–Stokes equations, boundary conditions are found to be critically important for accurately solving the coupled simulations. Following the idea of a regularized scheme (Latt *et al* 2008 *Phys. Rev.* E **77** 056703), a regularized boundary condition for solving a CDE is proposed. A simple extrapolation scheme is also proposed for the Neumann boundary condition. Spatial accuracies of three existing and the proposed boundary conditions are discussed in details. The numerical evaluations are based on simulations of steady and unsteady natural convection flows in a cavity and an unsteady Taylor–Couette flow. Our studies show that the simplest D2Q4 model with terms of $O(u)$ in the equilibrium distribution function is capable of obtaining results of equal accuracy as D2Q5 or D2Q9 models for the CDE. A slightly revised LB equation for solving a CDE that is used to cancel some unwanted terms does not seem to be necessary for incompressible flows. The regularized boundary condition for solving the CDE has second-order spatial accuracy and it is the best one in terms of the spatial accuracy. The regularized scheme and non-equilibrium extrapolation scheme are applicable to handle both the Dirichlet and Neumann boundary conditions. For the Neumann boundary condition with zero flux, all the five boundary conditions are applicable to give accurate results and the bounce-back scheme is the simplest one.

(Some figures in this article are in colour only in the electronic version)

1. Introduction

The lattice Boltzmann method (LBM) originated from the lattice gas automata [1] and has been developed as an alternative numerical scheme for solving the incompressible Navier–Stokes (NS) equations. In many applications, fluid flow problems are described by the NS equations coupled with a convection–diffusion equation (CDE). For example, the natural convection problem is described by the NS equations with a CDE for heat [2, 3]. A multiphase flow system can also be described by the NS equations and a Chan–Hilliard equation (a CDE) [4]. In a simple solute/solvent flow system, the solvent's motion is described by the NS equations and a CDE is used to describe the transport of the moving solute [5]. The NS equations coupled with two CDEs can be used to describe the temperature-sensitive ferrofluids system [6] and the melt flow in Czochralski crystal growth [7].

Often, hybrid solution schemes can be used to simulate flows governed by the NS equations and a CDE [3, 7]. For example, when simulating the natural convection, the fluid flow can be solved by LBM while the heat transfer governed by a CDE is solved by the finite difference method [3]. However, the hybrid scheme does not have good numerical stability [7]. Using LBM to solve both the NS and the CDE is appealing because of the simplicity of a consistent approach [2, 5, 8–11].

Many studies have applied LBM for solving flows governed by the NS equations and a CDE [2–6, 12]. Dawson *et al* [5] studied the solute/solvent flow using the D2Q7 model on the regular triangular lattice. However, the passive flow of solute described by a CDE is not coupled with the NS equation. Furthermore, in the study, only a periodic boundary is used and other boundary conditions are not used or evaluated. Niu *et al* [6] studied ferrofluids system and a common D2Q9 model is used for solving the CDE. But the relaxation time τ in the simulation for the CDE is held at 1 without justification. Recently, it was noted that some studies investigate LBM for a single CDE using the multiple-relaxation lattice Boltzmann method [13] or the lattice Bhatnagar–Gross–Krook method [14, 15]. Suga [14] studied the stability and accuracy of LBM when solving a single CDE but the study is based on a simple case and the effects of the boundary condition were not considered.

In some of the above studies [2, 5, 6], the terms of $O(u^2)$ are retained in the equilibrium distribution function (EDF). However, because the CDE does not involve second-order velocity terms, it has been argued that keeping the terms of $O(u)$ in EDF is sufficient [11, 15–17]. In this study we adopt this strategy. Besides the simplification, the common D2Q9 velocity model can be further simplified to a D2Q5 model in the two-dimensional (2D) case [4, 11, 12, 14, 18, 19].

In some studies [12, 18] using a D2Q5 LB model to solve a CDE, the weighting factors before the EDF seem random. Recently, Zheng *et al* [4] suggested a formula for the weighting factors. Here the theoretical difference between these models [4, 12, 18] would be analyzed. Through derivation procedures from the LB equation to a CDE, the constraints for the weighting factors in the EDF for these velocity models can be obtained [19].

Although Zheng *et al* [4] suggested a formula for the weighting factors, the accuracy of the scheme employing those factors was not evaluated. Whether the scheme [4] is numerically better than other D2Q5 and/or D2Q4 models [10, 13] is an open question. Furthermore, the boundary conditions for a CDE were not studied.

The boundary condition treatment is an important issue in the development of accurate LBM models. Many boundary conditions have been proposed for the LB method when it is applied to solve the NS equations [20–24]. However, there is comparatively little study of the boundary conditions for a CDE when it is coupled with the NS equations [25]. The equilibrium distribution scheme [22] used for the Dirichlet boundary in [25] looks correct

but seems to be unable to produce the correct heat flux near the heated wall. Here, based on the idea of the regularized distribution function [26], a regularized boundary condition for solving a CDE is proposed. A simple distribution extrapolation scheme is also proposed for the Neumann boundary condition. The accuracy of five boundary conditions including the proposed ones for solving a CDE will be evaluated.

In this paper, firstly the theory of the D2Q9, D2Q5 and D2Q4 models for the CDE is introduced. Then, to test the numerical accuracy and stability of these models, two typical flows described by NS equations and a CDE are investigated. In the numerical studies, the effects of the boundary condition are discussed in detail.

2. LB methods

2.1. Lattice Boltzmann method for NS equations

The NS equations and CDE are solved by two sets of particle distribution functions: $f_i(\mathbf{x}, t)$ and $g_i(\mathbf{x}, t)$, respectively. If there are more CDEs, additional particle distribution functions would be used. In our study, the incompressible NS equation is solved by maintaining a low Mach number in a common lattice BGK equation:

$$f_i(\mathbf{x} + \mathbf{e}_i\delta_t, t + \delta_t) - f_i(\mathbf{x}, t) = -\frac{1}{\tau_f}\left(f_i - f_i^{\mathrm{eq}}\right) + R_i(\mathbf{x}, t), \tag{1}$$

where $R_i(\mathbf{x}, t)$ is a forcing term added on the right-hand side of the lattice Boltzmann equation (LBE) to mimic the body force appearing in the NS equations. The relaxation parameter τ_f is related to the kinematic viscosity by $\nu = c_s^2(\tau_f - 0.5)\delta_t$, where $c_s = \frac{c}{\sqrt{3}}$ and $c = \frac{\delta_x}{\delta_t}$ is the ratio of lattice spacing δ_x and time step δ_t. In equation (1), $\mathbf{e}_i$ are the discrete velocities. For the D2Q9 model we used here, they are given by

$$[\mathbf{e}_0, \mathbf{e}_1, \mathbf{e}_2, \mathbf{e}_3, \mathbf{e}_4, \mathbf{e}_5, \mathbf{e}_6, \mathbf{e}_7, \mathbf{e}_8] = c \cdot \begin{bmatrix} 0 & 1 & 0 & -1 & 0 & 1 & -1 & -1 & 1 \\ 0 & 0 & 1 & 0 & -1 & 1 & 1 & -1 & -1 \end{bmatrix}.$$

The equilibrium distribution function (EDF) is defined as

$$f_i^{\mathrm{eq}}(\mathbf{x}, t) = \lambda_i \rho \left[1 + \frac{e_{i\alpha}u_\alpha}{c_s^2} + \frac{u_\alpha u_\beta}{2c_s^2}\left(\frac{e_{i\alpha}e_{i\beta}}{c_s^2} - \delta_{\alpha\beta}\right)\right]. \tag{2}$$

For the D2Q9 model, the weighting factors $\lambda_i = 4/9$ $(i = 0)$, $\lambda_i = 1/9$ $(i = 1, 2, 3, 4)$, $\lambda_i = 1/36$ $(i = 5, 6, 7, 8)$. In this paper, the Einstein summation convention is adopted.

The density ρ and velocity u_α are calculated from the hydrodynamic moments of the particle distribution functions [27]:

$$\rho = \sum_i f_i = \sum_i f_i^{\mathrm{eq}}, \qquad \rho u_\alpha = \sum_i e_{i\alpha} f_i + \frac{1}{2}F_\alpha\delta_t. \tag{3}$$

To recover the NS equations with a body force F_α, R_i is written in a fixed form: $R_i = \left(1 - \frac{1}{2\tau_f}\right)\frac{F_\alpha(e_{i\alpha} - u_\alpha)}{RT} f_i^{\mathrm{eq}}$ [27].

The no-slip boundary conditions can be handled by the momentum exchange scheme [21], the equilibrium distribution scheme [22], bounce-back or modified bounce-back [23], or the regularized scheme [26]. Here in our study, the boundary condition for solving the LB fluid is not our focus. Since the modified bounce-back scheme is of second-order spatial accuracy [23], it was adopted to handle the no-slip boundary. In that scheme, collision and forcing still occur at boundary nodes, which is also consistent with the momentum exchange scheme [21]. For the four corner points in our simulations, the scheme proposed by Zou

and He [24] was applied. For example, in the left lower corner point **x**, the unknown distribution functions f_1, f_2, f_5, f_6 and f_8 are obtained from $f_1 = f_3$, $f_2 = f_4$, $f_5 = f_7$ and $f_6 = f_8 = 0.5(\rho(\mathbf{x}+\mathbf{e}_5) - f_0 - 2(f_3 + f_4 + f_7))$. This is implemented just after the streaming step and before the collision steps. We do not intend to discuss the no-slip boundary condition intensively. One of our goals is to evaluate the boundary conditions for solving a CDE in the following section.

2.2. *Lattice Boltzmann methods for CDE*

Luo has shown that the LB equation can be derived from the Boltzmann equation [28]. Because the hydrodynamic moments of f_i^{eq} can be evaluated by the quadrature formula, the 2D velocity space ξ is discretized into several finite velocities $\mathbf{e}_i$ [28]. Usually to mimic the 2D NS equations, the D2Q9 velocity model with nine velocities is necessary for a Cartesian coordinate lattice [28]. However, to recover a CDE, the derivation from the LBE to the CDE shows that fourth-order isotropic lattice tensors are not required (refer to appendix A). Hence, models with fewer velocities, e.g. D2Q5 and D2Q4 [10, 11, 13–15, 19], can be used.

In our study, a typical CDE is written as

$$\partial_t T + \partial_\beta (u_\beta T) = k \partial_\beta (\partial_\beta T) + G, \tag{4}$$

where T is the macro-variable in the CDE, k is a constant controlling the diffusion and G is a source term.

In many studies [2, 5, 6, 16, 25], when the LB method is used to solve a CDE, a common LBE in the form of equation (5) is used:

$$g_i(\mathbf{x} + \mathbf{e}_i \delta t, t + \delta t) - g_i(\mathbf{x}, t) = \frac{1}{\tau_g}\left[g_i^{\mathrm{eq}}(\mathbf{x}, t) - g_i(\mathbf{x}, t)\right] + \delta_t S_i. \tag{5}$$

In equation (5), S_i is a source term used to recover the source term G in equation (4). The EDF, g_i^{eq}, has different forms in the studies referenced above.

The EDF of f_i^{eq} relevant to NS equations (i.e. equation (2)) involves terms of $O(u^2)$. For solving a CDE, Chopard *et al* [15] discussed about the presence of the $O(u^2)$ terms in the local equilibrium in detail. A term $O(u^2)$ is present as a correction to the diffusion coefficient, whether or not terms $O(u^2)$ are included in the local equilibrium distribution [15]. So the best way to be sure that the lattice Boltzmann model works fine is to assume $u$small enough so that any $O(u^2)$corrections can be safely ignored [15].

In the EDF of the following models, only terms of $O(u)$ are retained. For this strategy, through Chapman expansions we can see that there is an unwanted term $\delta t(\tau_g - 0.5)\partial_t\left[\partial_\beta\left(T u_\beta\right)\right]$ [15]. In our simulations, the flows are incompressible, which means $\partial_\beta u_\beta = 0$. Hence, the unwanted term is $\delta t(\tau_g - 0.5)\partial_t(u_\beta \partial_\beta T)$. For the steady incompressible flow, finally this unwanted term would be zero. For the unsteady incompressible flow, compared to the diffusion term in equation (4), the unwanted term is of order $O\left(\frac{u^2}{c_s^2}\right)$ [15]. Because in the simulations of incompressible flows, usually $\frac{u}{c_s} < 0.1$, the unwanted term is a higher order term and can be neglected.

In the study of Huber *et al* [18], $g_i^{\mathrm{eq}} = W_i T\left[1 + \frac{\mathbf{e}_i \cdot \mathbf{u}}{c_s^2}\right]$, where $\mathbf{e}_0 = (0, 0)$, $\mathbf{e}_i = (\cos(i-1)\pi/2, \sin(i-1)\pi/2)\cdot c$, $i = 1, 2, 3, 4$. The weighting factor $W_0 = 1/3$ and $W_i = 1/6$, $i = 1, 2, 3, 4$. Hence, the formula of the EDF can be written as $g_i^{\mathrm{eq}} = W_i T + \frac{T}{2}(\mathbf{e}_i \cdot \mathbf{u})$ due to $\mathbf{e}_0 = (0, 0)$. In the study of Chen *et al* [12], the EDF $g_i^{\mathrm{eq}} = \frac{T}{5} + \frac{T}{2}(\mathbf{e}_i \cdot \mathbf{u})$, $i = 0, 1, 2, 3, 4$.

However, in appendix A, we show that the general formula for the EDF is

$$g_i^{(0)} = H_i T + \frac{T e_{i\alpha} u_\alpha}{2} \tag{6}$$

with $H_0 = 1 - 2\eta$, $H_i = \frac{1}{2}\eta$, $i = 1, 2, 3, 4$, where $\eta \in (0, 0.5]$ is a free, positive parameter. We noted that when $\eta = 0.5$, equation (6) becomes a D2Q4 model formula [10, 13]. The diffusion coefficient $k = \eta(\tau_g - 0.5)\delta t$.

Later, Zheng *et al* applied a slightly revised LBE to solve a CDE which is Galilean invariant [4], which means the unwanted term can be canceled. The LBE reads

$$g_i(\mathbf{x} + \mathbf{e}_i\delta t, t + \delta t) - g_i(\mathbf{x}, t) = (1 - q)[g_i(\mathbf{x} + \mathbf{e}_i\delta t, \delta t) - g_i(\mathbf{x}, t)] + \frac{1}{\tau_g}\left[g_i^{\mathrm{eq}}(\mathbf{x}, t) - g_i(\mathbf{x}, t)\right], \tag{7}$$

where $q \in (0, 1]$ is a parameter related to the relaxation time τ_g. When $q = 1$, equation (7) is identical as the common LBE. Appendix A shows that the unwanted term $\delta t(\tau_g - 0.5)\partial_t[\partial_\beta(Tu_\beta)]$ can be canceled if using this LBE. However, in the above analysis, it has been shown that this unwanted term is of higher order and can be neglected in incompressible flows. Hence, this revised LBE might not be necessary. Through Chapman–Enskog expansions (appendix A), one can find that the EDF formula for equation (7) involves the parameter q and is slightly different from the above EDF (equation (6)). It is

$$g_i^{(0)} = H_i T + C_i T e_{i\alpha} u_\alpha, \tag{8}$$

with $C_i = \frac{1}{2q}$, $H_0 = 1 - 2\eta$, $H_i = \frac{1}{2}\eta$ $(i \neq 0)$for the D2Q5 or D2Q4 ($\eta = 0.5$) model. $\eta \in (0, 0.5]$ is a free, positive parameter. The diffusion coefficient $k = \eta\left(\tau_g q^2 - \frac{q}{2}\right)\delta t$, where $q = \frac{1}{\tau_g + 0.5}$.

2.3. *Boundary conditions for the CDE*

The boundary conditions for the CDE are important. For solving the LB fluid (NS equations), there are several types of boundary conditions available in literatures [20, 23, 26]. Whether they are applicable for solving a CDE and how they affect the accuracy is not clear. One of our goals in this paper is to evaluate the effects of the boundary condition. The five boundary conditions labeled from (i) to (v) are introduced in what follows.

(i) *Regularized scheme* (BC1). Here a regularized boundary condition for solving a CDE is proposed following the idea of the regularized scheme [26]. First let us suppose the streaming step is implemented, i.e. $g_i(\mathbf{x} + \mathbf{e}_i\delta t, t + \delta t) = g_i^+(\mathbf{x}, t)$, where g_i^+ is the post-collision value. The basic idea of the scheme is that $g_i = g_i^{\mathrm{eq}} + g_i^{\mathrm{neq}}$ is replaced by $\bar{g}_i = g_i^{\mathrm{eq}} + g_i^{(1)}$ and here$g_i^{(1)}$ is reconstructed as $g_i^{(1)} = B_\alpha e_{i\alpha}/2$, where $B_\alpha = \sum_i e_{i\alpha} g_i - Tu_\alpha$ for the D2Q4 or D2Q5 model with the common LBE. Then the collision is implemented as $g_i^+ = g_i^{\mathrm{eq}} + \left(1 - \frac{1}{\tau_g}\right)g_i^{(1)}$. Obviously, this construction ensures that $g_i^{(1)} = -g_{\mathrm{opp}(i)}^{(1)}$, where opp$(i)$ means the opposite direction of e_i. This is slightly different from the regularized scheme [26] for solving NS equations, which requires $f_i^{(1)} = f_{\mathrm{opp}(i)}^{(1)}$. That is because the second-order moments of the non-equilibrium distribution function are not required in Chapman–Enskog expansions from the LBE to CDE.

As we know, when the CDE is coupled with the NS equations, variable Tu_α is not evaluated as $\sum_i e_{i\alpha} g_i$ in the LBM code, because usually ρu_α is evaluated as $\sum_i f_i e_{i\alpha}$. Hence, usually $\sum_i \mathbf{e}_i g_i^{(1)} \neq 0$. From appendix A with $q = 1$, we know that $\sum_i e_{i\alpha} g_i^{(1)} = -\tau_g\left[\partial_t\left(Tu_\alpha\right) + \partial_\alpha\left(\eta T\right)\right]$. Hence $B_\alpha = \sum_i e_{i\alpha} g_i - Tu_\alpha$ possess unsteady information and knowledge of gradients of T.

For a boundary node, the macro-variables T, can be specified but there is one (D2Q5 or D2Q4 velocity models) or more unknown distribution functions after the streaming step. Hence, $B_\alpha = \sum_i e_{i\alpha} g_i - T u_\alpha$ is unknown because some g_i are unknown. In [26], the unknowns are obtained by 'bounce back of off-equilibrium parts' [24] because in their construction $f_i^{(1)} = f_{\mathrm{opp}(i)}^{(1)}$ is required. However, in our construction for a CDE, $g_i^{(1)} = -g_{\mathrm{opp}(i)}^{(1)}$ is required. Here we proposed an idea of 'bounce back of opposite value of off-equilibrium parts', i.e. the unknowns are obtained from $g_i = g_i^{\mathrm{eq}}(T, u) - \left(g_{\mathrm{opp}(i)} - g_{\mathrm{opp}(i)}^{\mathrm{eq}}\right)$. Then the reconstruction and collision steps at boundary nodes can be implemented.

(ii) *Simple extrapolation scheme* (BC2). Besides the regularized scheme, a simple extrapolation scheme for the Neumann boundary with the zero flux is also proposed as follows. The unknowns g_4 at boundary nodes $(i, j_{\max})$ on the upper wall are obtained through

$$g_4^+(i, j_{\max}) = \left(4g_4^+(i, j_{\max} - 1) - g_4^+(i, j_{\max} - 2)\right)/3, \tag{9}$$

where (i, j) is the horizontal and vertical index of the node in the computational domain.

(iii) *Non-equilibrium extrapolation scheme* (BC3). The non-equilibrium extrapolation scheme means that the collision process on the boundary node is still implemented with the non-equilibrium distribution function obtained through extrapolation from the nearest-neighbor fluid nodes [20]. For example, the unknowns $g_4^+(i, j_{\max})$ at boundary nodes on the upper wall is evaluated as

$$g_4^+(i, j_{\max}) = g_4^{\mathrm{eq}}(i, j_{\max}) + (1 - 1/\tau_g)(g_4(i, j_{\max} - 1) - g_4^{\mathrm{eq}}(i, j_{\max} - 1)). \tag{10}$$

(iv) *Simple bounce-back scheme* (BC4). The simple bounce back used here means the standard collision process does not occur on the boundary [23]. For example, the unknowns $g_4^+(i, j_{\max})$ at boundary nodes on the upper wall is evaluated as

$$g_4^+(i, j_{\max}) = g_2(i, j_{\max}). \tag{11}$$

The boundary condition usually used to mimic the non-slip boundary condition when solving NS equations. Here the scheme may be valid for a Neumann boundary condition with zero flux.

(v) *Equilibrium scheme* (BC5). For a Dirichlet boundary condition, an available practice is to assign the equilibrium distribution to the distribution functions at a boundary node [22]. For a Neumann boundary condition, after the macro-variable T is extrapolated, the equilibrium distribution can be assigned to the distribution functions at a boundary node.

3. Numerical study

In this section we make a comparison between D2Q9, D2Q5 and D2Q4 models for a CDE when it is coupled with the NS equations. Two typical flows are investigated. One is the steady and unsteady natural convection in a square cavity and the other is a swirling flow, the Taylor–Couette flow. The accuracy and stability of these models are evaluated.

3.1. Steady and unsteady natural convection in a square cavity

The momentum and thermal boundary conditions for a natural convection are illustrated in figure 1. The temperatures on the left and right walls are T_1 and T_2, respectively, where $T_1 > T_2$. The temperature difference induces natural convection in the cavity. The upper and lower walls are adiabatic. The Boussinesq approximation is applied to the buoyancy force term.

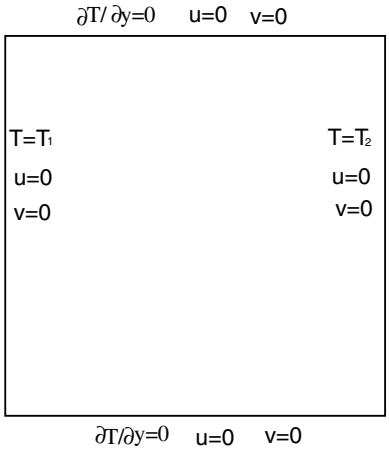

Figure 1. Momentum and thermal boundary conditions for natural convection in a square cavity.

The thermal expansion coefficient β and kinematic viscosity ν are considered as constants, and the buoyancy term is assumed to depend linearly on the temperature, $F_y = \rho\beta g\,(T - T_0)$, where g is the acceleration due to gravity and $T_0 = (T_1 + T_2)/2$ is the average temperature which is also used as the initial condition. The external body force in the y direction appears in the NS equations.

The dynamical similarity depends on two dimensionless parameters: the Prandtl number Pr and the Rayleigh number Ra defined as

$$Pr = \nu/k, \tag{12}$$

$$Ra = \beta g\,(T_1 - T_2)\,L^3/\nu k, \tag{13}$$

where k is the thermal diffusivity. In our simulations, $Pr = 7$. A characteristic velocity was defined as $U_c = \sqrt{\beta g\,(T_1 - T_2)\,L}$, where L is the length of the cavity. Two relaxation times τ_f and τ_g are determined by $\nu$and k, respectively. For example, when τ_f is determined, then for the D2Q4 CDE model, the $\tau_g = k/(\eta\delta_t) + 0.5 = 2c_s^2\left(\tau_f - 0.5\right)/(\mathrm{Pr}) + 0.5$ (refer to appendix A with $q = 1$ and $\eta = 0.5$). A grid-resolution study shows that a computational domain with 101×101 lattice nodes is sufficient to get accurate results. Hence in this section, the grid size used is 101×101. For the steady-flow simulation the convergence criterion is $\frac{\sum_{i,j}\|\mathbf{u}(t+500)-\mathbf{u}(t)\|^2}{\sum_{i,j}\|\mathbf{u}(t)\|^2} < 10^{-8}$, where the summation is over the entire system. In the following section, the D2Q4 with different boundary conditions will be evaluated.

In this section, we would focus on the effect of the boundary condition for the CDE. The existing and proposed boundary conditions would be applied and evaluated.

LBM simulation results using different boundary conditions are compared with the benchmark solution [29] for $Ra = 10^5$ and $Pr = 0.71$. Here the D2Q4 velocity model [10, 13] is used to solve the CDE. In table 1, the first and second rows (labeled 'BC') indicate the boundary conditions used for the left/right and the upper/lower boundaries, respectively. In the table, $u_{\max}$ is the maximum horizontal velocity on the vertical mid-plane of the cavity and $v_{\max}$ is the maximum vertical velocity on the horizontal mid-plane of the cavity. $|\psi_{\mathrm{mid}}|$ and $|\psi_{\max}|$ are absolute values of the stream function at the mid-point of the cavity and the maximum stream function, respectively. The stream function is normalized by the thermal

Table 1. Comparison between LBM results using different boundary conditions and the benchmark solution [29] for $Ra = 10^5$, $Pr = 0.71$.

	Case 1	Case 2	Case 3	Case 4	Case 5	Case 6	Case 7	Case 8	Davis [29]
BC	BC5 BC4	BC1 BC1	BC1 BC2	BC1 BC3	BC1 BC4	BC1 BC5	BC3 BC2	BC3 BC4	–
τ_f	0.7398	0.5799	0.5799	0.5799	0.5799	0.5799	0.5799	0.5799	–
$\lvert\psi_{\text{mid}}\rvert$	9.171	9.096	9.094	9.097	9.091	9.097	9.099	9.095	9.111
$\lvert\psi_{\max}\rvert$	9.706	9.619	9.616	9.625	9.607	9.625	9.626	9.611	9.612
$u_{\max}$	35.92	34.94	34.91	34.99	34.75	34.95	34.98	34.76	34.73
$v_{\max}$	69.78	68.52	68.50	68.54	68.46	68.57	68.61	68.52	68.59
$\overline{Nu}$	4.612	4.505	4.504	4.498	4.506	4.508	4.510	4.514	4.519
$Nu_{1/2}$	4.629	4.497	4.496	4.487	4.497	4.503	4.502	4.505	4.519
Nu_0	3.383	4.549	4.549	4.560	4.532	4.553	4.562	4.540	4.509

BC1: regularized scheme.
BC2: simple extrapolation.
BC3: non-equilibrium extrapolation [20].
BC4: simple bounce-back [23].
BC5: equilibrium scheme [22].

diffusivity k. The Nusselt numbers at the heated end Nu_0 and at the centerline of the cavity $Nu_{1/2}$ were also evaluated. The Nusselt number is defined as

$$Nu = \frac{1}{k\,(T_1 - T_2)} \int_0^L \left(uT - k\frac{\partial T}{\partial x} \right) \mathrm{d}y. \tag{14}$$

The average Nusselt number in the whole flow domain $\overline{Nu}$ is also listed. For the temperature gradient in equation (14), it is evaluated by a central difference except for nodes on the left/right boundary. For the nodes on the boundary the gradient was evaluated by a biased difference. For example, on the left wall, $\frac{\partial T}{\partial x} = T(i_{\min} + 1, j) - T(i_{\min}, j)$.

From table 1 we see that in case 1, the equilibrium scheme (BC5) [22] $g_i = g_i^{\text{eq}}$ is applied on left/right boundaries. The scheme seems to be able to correctly capture the overall characteristics of the flow, the average Nu, the maximum absolute value of the stream function $|\psi_{\max}|$, etc. [25]. However, the heat flux near the heated wall is considerably different from the benchmark solution. On the other hand, other cases except case 1 show that the BC1, BC3 for the Dirichlet boundary (left/right boundaries) is free of that problem and accurate results can be obtained.

For the upper/lower Neumann boundary condition with zero flux, all five boundary conditions are applicable. The BC2 and BC4 can be implemented straightforward but BC1, BC2 and BC5 require the macro-variable T value at boundary nodes which can be extrapolated from inner fluid nodes. From table 1, it is found that all five schemes are able to give accurate results.

The spatial accuracy is also evaluated in figure 2. It shows the numerical errors as a function of the grid resolution. In all simulations, all parameters are fixed except τ_f,$\tau_g$which change with the grid resolution. The error is defined as the absolute value of the difference between the final steady value of $\overline{Nu}$ for the result of 400 × 400 and that of each resolution. The slopes of the fitted lines are also labeled. They demonstrate that the LBM has around second-order spatial accuracy. The regularized boundary condition for solving the CDE is the best one in terms of the spatial accuracy. The combination of boundary conditions BC3+BC2

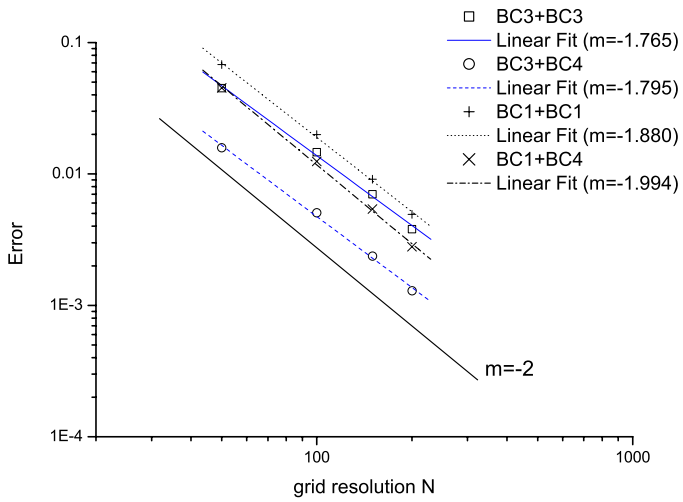

Figure 2. Error of $\overline{Nu}$ as a function of grid resolution using different combinations of boundary conditions. The first and second boundary condition types in labels denote the boundary conditions applied to the left/right and upper/lower boundary, respectively. A line of slope -2 is drawn to guide the eye. m is the slope of a line.

is also evaluated but the spatial accuracy is about 1.573 that means the BC2 is not so good and it slightly decreases the second-order spatial accuracy of the LBM.

For the stability of these boundary conditions, we did not find a significant difference between them. For example, when the grid resolution is fixed as 100×100, the $Pr = 0.71$, $T_1 - T_2 = 1$ and $U_c = 0.1$, for all these combinations of boundary conditions the maximum Ra that can be reached before numerical instabilities appear is about 4×10^6.

It is also worth mentioning that when the relaxation time τ_g in the simulation for the CDE is taken to be unity [6], the equilibrium scheme (BC5) is identical to the non-equilibrium extrapolation scheme (BC3) [20]. That is why the equilibrium distribution scheme can also give accurate results when $\tau_g = 1$. For case 1 in table 1, if τ_g is taken to be unity, the result would be better.

For numerical efficiency, our numerical study shows that when solving a single CDE, for a same case, the CPU time using D2Q9, D2Q5 and D2Q4 are 137 s, 96 s and 83 s, respectively. Noted the D2Q9 also omitted the terms of $O(u^2)$ in EDF. Hence, for solving a single CDE, the D2Q4 model saves about 13.5% CPU time compared with the D2Q5 model. Our simulations suggested for solving the NS-CDE coupled system, such as a case in table 1; the CDE solution takes about 21.9% of the total CPU time. Hence, using the D2Q4 model for the CDE saves about $21.9\% \times 13.5\% = 3.0\%$ of the total CPU time compared with that using the D2Q5 model. Our simulation do confirmed the estimation.

In the above, the D2Q4 model with different boundary conditions is evaluated. To evaluate the D2Q9 and D2Q5 models more accurately, an unsteady natural convection with $Ra = 280\,000$ and $Pr = 7$ is investigated. To make a comparison, a finite volume method (FVM), i.e. SIMPLE algorithm, is used to obtain a benchmark solution. A fine mesh 200×200 is used and the non-dimensional time step is $t* = tk/h^2 = 0.0001$. At each time step, the residuals of the momentum equation and energy equation are all assured to be converged to 10^{-6}.

Table 2. Comparison between LBM results and FVM results for natural convection with $Ra = 280\,000$ and $Pr = 7$.

Case	Model	η	τ_f	τ_g	Error
1	D2Q9	–	0.7121	0.5301	0.0084
2	D2Q5	0.4	0.7121	0.5253	0.0065
3	D2Q4	0.5	0.7121	0.5202	0.0060
4	D2Q5	0.3333	0.7121	0.5300	0.0068
5	D2Q5 [4]	0.0834	0.7121	1.2000	0.0092
6	D2Q5 [4]	0.3338	0.7121	0.5692	0.0086
7	D2Q5 [4]	0.4454	0.7121	0.5500	0.0080

In the LBM simulations, BC1 and BC4 are applied to the left/right and upper/lower boundary, respectively. The grid resolution is 100×100. As an example, the streamlines and isotherms obtained from case 6 in table 2 are illustrated in figure 3. The stream function obtained from LBM agrees well with that obtained from the FVM at $t* = 0.009$, 0.015, 0.09. Initially, there is no flow in the cavity. The isotherms are also highly consistent with those obtained from FVM except for some very small differences near the upper and lower boundaries. Similar results are obtained for all of the cases in table 2.

Figure 4 shows the Nusselt numbers for case 6 at the heated end, Nu_0, and at the centerline of the cavity, $Nu_{1/2}$, as functions of time. The LBM result agrees well with that of FVM. It demonstrates that a strong internal wave motion survived for several periods of $O(0.01)$, which is highly consistent with the results in [30].

To further check the accuracy of the D2Q4, D2Q5 and D2Q9 models, the error of the Nusselt number $Nu_{1/2}$ between LBM and the benchmark FVM solution was evaluated. The error is defined as

$$\text{Error} = \sum_{t_i^*} \left| \left(Nu_{1/2}(t_i^*)\right)_{\text{LBM}} - \left(Nu_{1/2}(t_i^*)\right)_{\text{FVM}} \right| \Big/ \sum_{t_i^*} \left(Nu_{1/2}(t_i^*)\right)_{\text{FVM}}, \tag{15}$$

where $\left(Nu_{1/2}(t_i^*)\right)_{\text{LBM}}$, $\left(Nu_{1/2}(t_i^*)\right)_{\text{FVM}}$ means $Nu_{1/2}$ obtained from LBM and FVM, respectively, at the non-dimensional time t_i^*. The summation is taken over 40 temporal points from $t_i = 0.001$ to $t_i = 0.04$ with an interval of 0.001. Table 2 shows the error of different LBM models. It can be seen from table 2 that the errors of different LBM models are of the same order. No one model seems significantly better than any other.

Regarding numerical stability, the simulations are found to be still stable when the minimum relaxation time $\tau_f = 0.5106$ and the corresponding relaxation times in LBE for solving the CDE are $\tau_g = 0.501\,01$, $\tau_g = 0.501\,26$ and $\tau_g = 0.501\ 52$ for D2Q4, D2Q5 [12] and D2Q5 [18] models, respectively.

3.2. Unsteady Taylor–Couette flow

In this section, we consider the problems of the laminar axisymmetric swirling flow of an incompressible liquid with an axis in the x direction. The continuity equation (16) and Navier–Stokes momentum equations (17) in the pseudo-Cartesian coordinates (x,r) are used to describe the flow in the axial and radial directions [31]:

$$\partial_\beta u_\beta = -\frac{u_r}{r} \tag{16}$$

$$\partial_t u_\alpha + \partial_\beta (u_\beta u_\alpha) + \frac{1}{\rho_0}\partial_\alpha p - \nu \partial_\beta^2 u_\alpha = -\frac{u_\alpha u_r}{r} + \frac{\nu}{r}\left(\partial_r u_\alpha - \frac{u_r}{r}\delta_{\alpha r}\right) + \frac{u_\theta^2}{r}\delta_{\alpha r}. \tag{17}$$

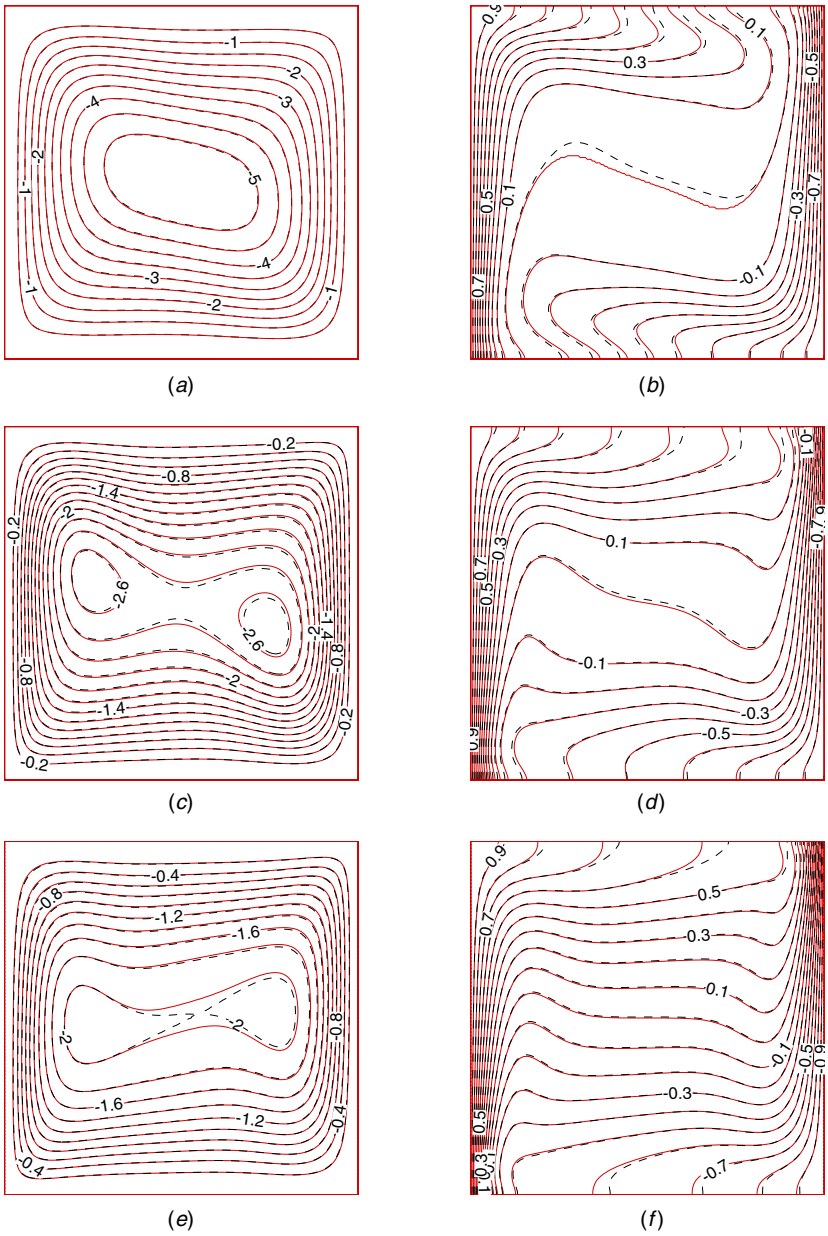

Figure 3. Numerical results for unsteady natural convection with $Ra = 280\,000$ and $Pr = 7$. Solid lines and dashed lines are results obtained from FVM and LBM, respectively. (*a*), (*b*) Streamlines and isotherms at $t^* = 0.009$; (*c*), (*d*) streamlines and isotherms at $t^* = 0.015$; (*e*), (*f*) streamlines and isotherms at $t^* = 0.09$. The stream function here is normalized by the kinematic viscosity ν. Temperature is normalized as $T^* = 2(T - T_0)/(T_1 - T_2)$, it changes from +1 on the left wall to -1 on the right wall. The contour interval in (*a*), (*c*) and (*e*), and (*b*), (*d*) and (*f*) are -0.5, -0.2 and -0.1, respectively.

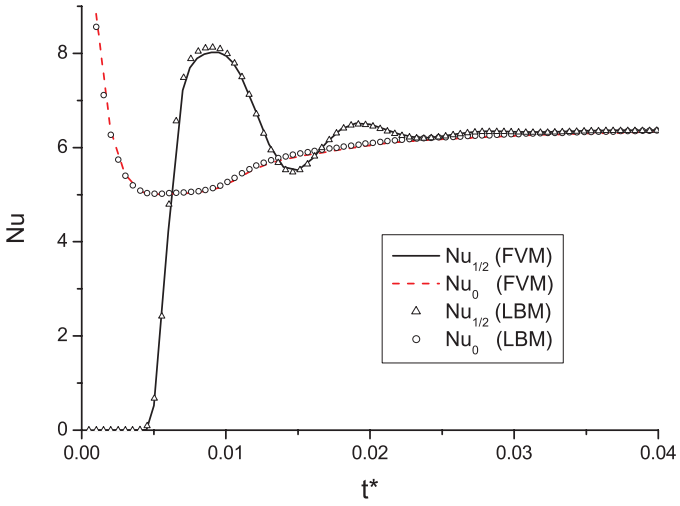

Figure 4. The Nusselt number $Nu_{1/2}$ and Nu_0 for case 6 as a function of non-dimensional time t^*.

In the above equations, u_α, u_β (α,β represent x or r) are the axial or radial component of velocity.

For the axisymmetric swirling flow, there are no circumferential gradients but there may still be the non-zero swirl velocity u_z. The momentum equation of azimuthal velocity is

$$\partial_t u_\theta + \partial_\alpha (u_\alpha u_\theta) = \nu \partial_\beta (\partial_\beta u_\theta) + \frac{\nu}{r}\left(\partial_r u_\theta - \frac{u_\theta}{r}\right) - \frac{2u_r u_\theta}{r}. \tag{18}$$

Obviously, it is a CDE with a source term $G = \frac{\nu}{r}\left(\frac{\partial u_\theta}{\partial r} - \frac{u_\theta}{r}\right) - \frac{2u_r u_\theta}{r}$. The flows studied here are incompressible, and hence the u_x and u_r usually should satisfy the constraints $u_x/c_s \leqslant 0.1$ and $u_r/c_s \leqslant 0.1$.

Figure 5 illustrates the geometry and boundary conditions for the Taylor–Couette flow. The radius ratio of the inner cylinder to the outer cylinder is set as 0.5 and the aspect ratio is set as 3.8. The computational domain is in the $x - r$ plane and the governing equations for the flow are equations (16)–(18). The Reynolds number is defined as $Re = WD/\nu$, where W is the azimuthal or swirling velocity of the inner cylinder, D is the gap of the annulus, and ν is the kinematic viscosity. In this section, $Re = 100$ is investigated. Our simulations were initialized with zero velocities everywhere.

To mimic the additional axisymmetric contributions in the 2D Navier–Stokes equations (i.e. equations (16) and (17)) in cylindrical coordinates, the source term R_i in the LB equation (i.e. equation (1)) can be chosen as $R_i = \delta_t R_i^{(1)} + \delta_t^2 R_i^{(2)}$, where $R_i^{(1)}$ and $R_i^{(2)}$ are

$$R_i^{(1)} = \frac{-\omega_i \rho u_r}{r} \quad \text{and} \quad R_i^{(2)} = \frac{\omega_i}{c_s^2} e_{i\beta}\left[\frac{-\rho u_\beta u_r}{r} + \frac{\rho\nu}{r}\left(\partial_r u_\beta - \frac{u_r}{r}\delta_{\beta r}\right)\right] + \frac{\rho u_\theta^2}{r}\delta_{\alpha r}, \tag{19}$$

respectively [32, 33]. The velocity is evaluated through $\rho u_\alpha = \sum_i e_{i\alpha} f_i$ [33].

Adding a source term S_i into the LB equation (5), we can take the effect of the term 'G' in the azimuthal velocity-governing equation, i.e. equation (18). From appendix A, we obtained the two constraints $G = \sum_i S_i$ and $\sum_i e_{i\beta} S_i = 0$ on S_i. For simplicity, here G is evenly distributed in all velocity models, i.e. the source term $S_i = 0.2G$, $i = 0,1, 2, 3, 4$, for the D2Q5 model and $S_i = 0.25G$, $i = 1, 2, 3, 4$, for the D2Q4 model.

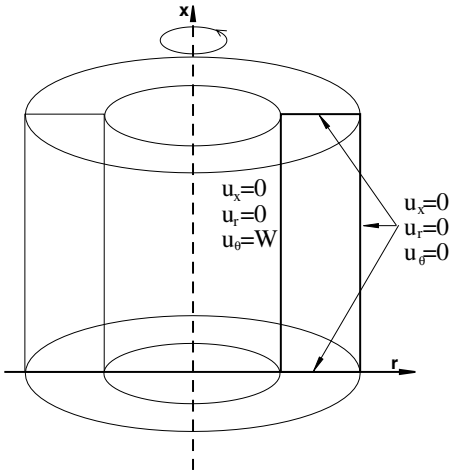

Figure 5. Boundary conditions for the Taylor–Couette flow.

Table 3. Results of the Taylor–Couette flow with different LBM models.

Case	LBM model	η	τ_f	τ_g	Error
1	D2Q9	–	0.62	0.62	0.013 10
2	D2Q5	0.4	0.62	0.6	0.005 99
3	D2Q4	0.5	0.62	0.58	0.003 48
4	D2Q5	0.3333	0.62	0.62	0.007 68
5	D2Q5 [4]	0.4507	0.62	0.8	0.004 31
6	D2Q5 [4]	0.32	0.62	1.5	0.004 04

Here we also used a FVM solution as a benchmark solution which is obtained from a fine mesh (50×190) and a small time step $\Delta t* = 0.001$. In this case, time is non-dimensionalized as $t* = t\nu/D^2$.

In the LBM simulations, a 40 × 152 uniform grid is used and non-equilibrium extrapolation (BC3) is applied for solving the CDE. The other parameters adopted are listed in table 3. The comparison between LBM and FVM for the stream function and swirling velocity for case 5 are illustrated in figure 6. From figure 6, we can see the evolution of the vortex and the final four-cell secondary mode. The LBM results obtained for case 5 agree well with the FVM solution.

To further check the accuracy of the D2Q4, D2Q5 and D2Q9 models, the error of the stream function $\psi_{\max}$ between LBM and the benchmark FVM solution in figure 7 was evaluated. The error is defined as

$$\text{Error} = \sum_{t_i^*} \left| \left(\psi_{\max}(t_i^*)\right)_{\text{LBM}} - \left(\psi_{\max}(t_i^*)\right)_{\text{FVM}} \right| \Bigg/ \sum_{t_i^*} \left(\psi_{\max}(t_i^*)\right)_{\text{FVM}}, \qquad (20)$$

where $\left(\psi_{\max}(t_i^*)\right)_{\text{LBM}}$, $\left(\psi_{\max}(t_i^*)\right)_{\text{FVM}}$ mean the stream functions obtained from LBM and FVM, respectively, at the non-dimensional time t_i^*. The summation is taken over 40 temporal points from $t_i^* = 0.02$ to $t_i^* = 0.80$ with an interval of 0.02. Table 3 shows the error of different LBM models. It shows that the errors of different LBM models are of the same order: no one model seems significantly better than any other.

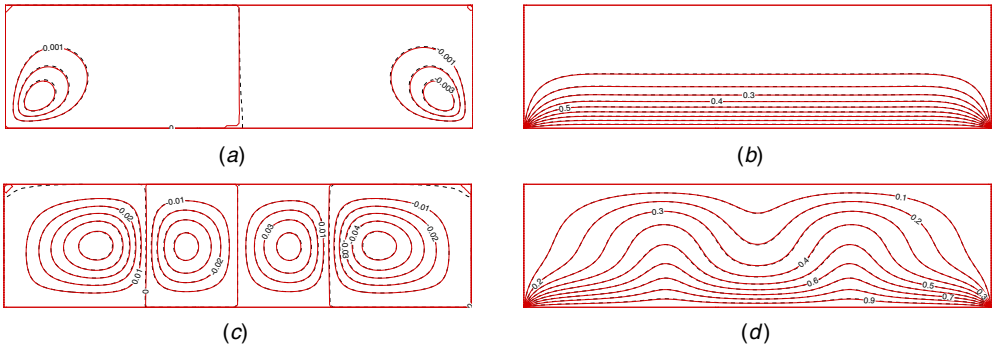

Figure 6. (*a*), (*b*) Streamlines and swirling velocity at non-dimensional time $t^* = 0.04$; (*c*), (*d*) streamlines and swirling velocity at $t^* = 0.8$. Solid lines and dashed lines are results obtained from FVM and LBM, respectively. Contour interval in (*a*)–(*d*) is -0.001, 0.1, -0.01 and 0.1, respectively. Swirling velocity u_θ is normalized by the characteristic velocity W. x axis in the horizontal direction.

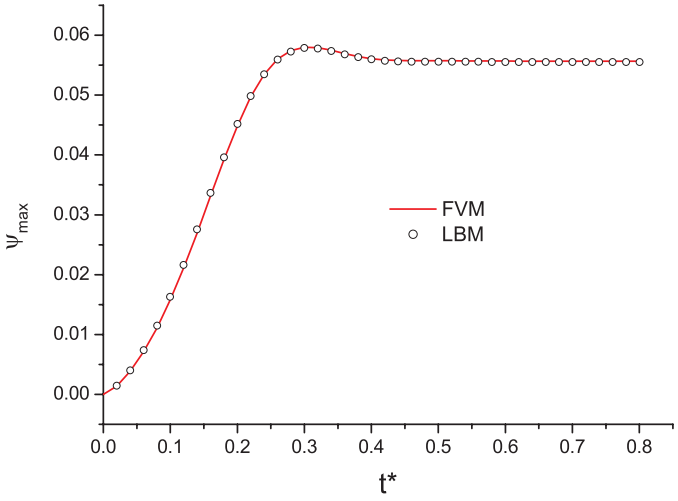

Figure 7. The maximum stream function in the flow field as a function of t^*.

4. Conclusion

Numerical simulations were carried out to evaluate the LB D2Q4 model and D2Q5 models with different weighting factors and the D2Q9 model. The simulations show that the performances of different models for solving a CDE in terms of accuracy and numerical stability are similar. The slightly revised LBE is not found to be better than the common LBE in terms of accuracy or numerical stability for these incompressible flow simulations. The D2Q4 model with terms of $O(u)$ in the EDF is the simplest scheme able to solve a CDE accurately.

Boundary conditions for the LBM CDE solution were also evaluated intensively. The spatial accuracy of the proposed regularized scheme is found to be closest to second order. When solving the CDE, the regularized scheme and non-equilibrium extrapolation scheme are applicable to handle both the Dirichlet and Neumann boundary conditions. For the Neumann

boundary condition with zero flux, all the five boundary conditions are applicable to give accurate results and the bounce-back scheme is the simplest one.

Acknowledgments

This work was supported by the National Science Foundation of China (NSFC, no 10802085) and the Innovation Project of the Chinese Academy of Sciences (grant no KJCX1-YW-21).

Appendix

In this section, we will show how a CDE can be recovered from a LB equation with D2Q9, D2Q5 or D2Q4 models. As a starting point, the following Taylor expansion and Chapman–Enskog expansions are adopted.

The Taylor expansion is $g_i(\mathbf{x}+\mathbf{e}_i\delta t, t+\delta t) = \sum_{n=0}^{\infty} \frac{\varepsilon^n}{n!} D^n g_i(\mathbf{x}, t)$ (A.1)

and the Chapman–Enskog expansion is $\begin{cases} g_i = g_i^{(0)} + \varepsilon g_i^{(1)} + \varepsilon^2 g_i^{(2)} + \cdots \\ \partial_t = \partial_{t0} + \varepsilon \partial_{t1} + \cdots \end{cases}$, (A.2)

where $\varepsilon = \delta t$ and $D \equiv (\partial_t + \mathbf{e}_\beta \cdot \partial_\beta)$, $\beta = x,y$.

When using second-order strategy to integrate the Boltzmann equation, the forcing term $S_i\left(\mathbf{x}+\frac{\mathbf{e}_i\delta_t}{2}, t+\frac{\delta_t}{2}\right)$ can be written as $S_i + \frac{\delta t}{2}\left(\partial_t + e_{i\beta}\partial_\beta\right) S_i$. Note that here the Taylor expansion is used. Hence, the LBE (i.e. equation (7)) is

$$\begin{aligned} &g_i\left(\mathbf{x}+\mathbf{e}_i\delta t, t+\delta t\right) - g_i\left(\mathbf{x}, t\right) \\ &= (1-q)[g_i\left(\mathbf{x}+\mathbf{e}_i\delta t, t\right) - g_i\left(\mathbf{x}, t\right)] + \tfrac{1}{\tau_g}\left[g_i^{\mathrm{eq}}\left(\mathbf{x}, t\right) - g_i\left(\mathbf{x}, t\right)\right] + \delta t \cdot S_i + \tfrac{(\delta t)^2}{2}\left(\partial_t + e_{i\beta}\partial_\beta\right) S_i. \end{aligned} \tag{A.3}$$

When $q = 1$, equation (A.3) is a common LBE with a source term. The equilibrium distribution function $g_i^{(0)}$ is constrained by the following relationships:

$$\sum_i g_i^{(0)} = T, \qquad \sum_i g_i^{(0)} e_{i\alpha} = \frac{T}{q} u_\alpha, \qquad \sum_i g_i^{(0)} e_{i\alpha} e_{i\beta} = E_{\alpha\beta}. \tag{A.4}$$

From the definition of the macro-variable $T = \sum_i g_i$, we can see that $\sum_i g_i^{(m)} = 0$ for $m > 0$. However, when the CDE is coupled with the NS equations, variable $\frac{T}{q}u_\alpha$ is not evaluated as $\sum_i e_{i\alpha} g_i$ in the LBM code (because usually ρu_α is evaluated as $\sum_i f_i e_{i\alpha}$). Hence, usually $\sum_i \mathbf{e}_i g_i^{(m)} \neq 0$ for $m > 0$.

Retaining terms up to $O(\varepsilon^2)$ in equations (A.1) and (A.2) and substituting into the LBE equation (A.3) results in the following equations:

$$O(\varepsilon^0) : \left(g_i^{(0)} - g_i^{\mathrm{eq}}\right)/\tau_g = 0, \tag{A.5}$$

$$O(\varepsilon) : \left(\partial_{t0} + q e_{i\beta}\partial_\beta\right) g_i^{(0)} = \frac{1}{\tau_g}\left(-g_i^{(1)}\right) + S_i, \tag{A.6}$$

$$\begin{aligned} O(\varepsilon^2) : \partial_{t1} g_i^{(0)} + (\partial_{t0} + q e_{i\beta}\partial_\beta) g_i^{(1)} + \tfrac{1}{2}\left[\partial_{t0}^2 + 2\partial_{t0}\left(e_{i\beta}\partial_\beta\right) + q e_{i\alpha}\partial_\alpha e_{i\beta}\partial_\beta\right] g_i^{(0)} \\ = \frac{1}{\tau_g}\left(-g_i^{(2)}\right) + \frac{1}{2}\left(\partial_{t0} + e_{i\beta}\partial_\beta\right) S_i. \end{aligned} \tag{A.7}$$

Summing on i in equation (A.6), we obtain at $O(\varepsilon)$

$$\partial_{t0} T + \partial_\beta \left(T u_\beta\right) = \sum_i S_i. \tag{A.8}$$

Then we proceed to $O(\varepsilon^2)$. Using equation (A.6) and substituting the $(\partial_{t0} + q e_{i\beta}\partial_\beta) g_i^{(0)}$ with $\frac{1}{\tau_g}\left(-g_i^{(1)}\right) + S_i$, through simple algebra, the left-hand side of equation (A.7) can be written as

$$\begin{aligned}
&(\partial_{t0} + q e_{i\beta}\partial_\beta) g_i^{(1)} + \frac{1}{2}\left[\partial_{t0}^2 + 2\partial_{t0}\left(e_{i\beta}\partial_\beta\right) + q e_{i\alpha}\partial_\alpha e_{i\beta}\partial_\beta\right] g_i^{(0)} \\
&= \left(1 - \frac{1}{2\tau_g}\right)\left(\partial_{t0} + q e_{i\beta}\partial_\beta\right) g_i^{(1)} + \frac{1}{2}\left(\partial_{t0} + q e_{i\beta}\partial_\beta\right) S_i + (1-q)\partial_{t0}\partial_\beta\left(e_{i\beta} g_i^{(0)}\right) \\
&\quad + \frac{q(1-q)}{2}\partial_\alpha\partial_\beta\left(e_{i\alpha} e_{i\beta} g_i^{(0)}\right).
\end{aligned} \tag{A.9}$$

Using equation (A.9) and summing on i in equation (A.7), we obtain at $O\left(\varepsilon^2\right)$

$$\begin{aligned}
&\partial_{t1} T + \left(1 - \frac{1}{2\tau_g}\right)\sum_i \left(\partial_{t0} + q e_{i\beta}\partial_\beta\right) g_i^{(1)} + \frac{(1-q)}{q}\partial_{t0}\partial_\beta\left(T u_\beta\right) + \frac{q(1-q)}{2}\partial_\alpha\partial_\beta\left(E_{\alpha\beta}\delta_{\alpha\beta}\right) \\
&\qquad = \left(\frac{1-q}{2}\right)\partial_\beta\left(\sum_i e_{i\beta} S_i\right).
\end{aligned} \tag{A.10}$$

Note that using equation (A.6) and the definition of macro-variables, we can obtain

$$\sum_i \left(\partial_{t0} + q e_{i\beta}\partial_\beta\right) g_i^{(1)} = -\tau_g \partial_{t0}\partial_\beta\left(T u_\beta\right) - \tau_g q^2 \partial_\beta\partial_\gamma\left(E_{\beta\gamma}\right) + \tau_g q \partial_\beta\left(\sum_i e_{i\beta} S_i\right). \tag{A.11}$$

Hence, equation (A.10) becomes

$$\begin{aligned}
&\partial_{t1} T + \left(\frac{1}{2} - \tau_g + \frac{1-q}{q}\right)\partial_{t0}\partial_\beta\left(T u_\beta\right) + \left(\frac{q}{2} - \tau_g q^2\right)\partial_\alpha\partial_\beta\left(E_{\alpha\beta}\right) \\
&\qquad = \left(0.5 - \tau_g q\right)\partial_\beta\left(\sum_i e_{i\beta} S_i\right).
\end{aligned} \tag{A.12}$$

Combining equations (A.8) and (A.12) leads to the following equation:

$$\begin{aligned}
&\partial_t T + \partial_\alpha (T u_\alpha) - \sum_i S_i \delta t \left\{\left[\frac{2-q}{2q} - \tau_g\right]\partial_t[\partial_\beta\left(T u_\beta\right)] + \left(\frac{q}{2} - \tau_g q^2\right)\partial_\alpha\partial_\beta(E_{\alpha\beta})\right. \\
&\qquad \left. -(0.5 - \tau_g q)\partial_\beta\left(\sum_i e_{i\beta} S_i\right)\right\} + O(\delta t^2) = 0.
\end{aligned} \tag{A.13}$$

$E_{\alpha\beta}$ in equation (A.4) is defined as $E_{\alpha\beta} = \eta T \delta_{\alpha\beta}$, where η is a constant to be determined later. To make equation (A.13) fully recover the convection–diffusion equation

$$\partial_t T + \partial_\alpha\left(T u_\alpha\right) - k\partial_\beta^2\left(T\right) + G + O(\delta t^2) = 0, \tag{A.14}$$

the coefficient before the term $\partial_t\left[\partial_\beta\left(T u_\beta\right)\right]$ in equation (A.13) should satisfy a constraint $\frac{2-q}{2q} - \tau_g = 0$. It gives $q = \frac{1}{\tau_g + 0.5}$.

In the meantime, the thermal diffusivity should be defined as $k = \left(\tau_g q^2 - \frac{q}{2}\right)\eta\delta t$. Here $\eta = k\big/[0.5q\left(1-q\right)\delta_t]$, $\tau_g > 0.5$, $0 < q < 1$. When $q = 1$, $\eta = k\big/\left[\left(\tau_g - 0.5\right)\delta_t\right]$.

The source term is required to satisfy two constraints $G = \sum_i S_i$ and $\sum_i e_{i\beta} S_i = 0$.

On the other hand, through the constraints in equation (A.4), we obtained the coefficients in the EDF $g_i^{(0)} = B_i T + C_i T e_{i\alpha} u_\alpha$ as

$$C_i = \frac{1}{2q}, \qquad B_0 = 1 - 2\eta, \qquad B_i = \frac{1}{2}\eta \qquad (i \neq 0). \tag{A.15}$$

It is noted that for the common D2Q9 model [28] with terms of $O(u^2)$ in the EDF, there is an extra term $(\tau_g - 0.5)\delta_t \cdot \partial_\gamma \left(\partial_\beta \left(T u_\beta u_\gamma\right)\right)$ in the CDE because in this case $\sum_i g_i^{(\mathrm{eq})} e_{i\beta} e_{i\gamma} = c_s^2 T \delta_{\beta\gamma} + T u_\beta u_\gamma$. That term is a higher order term and can be neglected.

There is an extra term $\left(0.5 - \tau_g\right) \partial_t \left[\partial_\beta \left(T u_\beta\right)\right]$ in the CDE (i.e. equation (A.14)) for D2Q5 models in [12, 18] due to $q = 1$. However, this term is of higher order than the convection or diffusion term in the CDE. We can neglect this term. Basically the D2Q5 model [4] would have the same accuracy as the common D2Q5 models [12, 18] with different weighting factors.

References

[1] McNamara G and Zanetti G 1988 Use of the Boltzmann equation to simulate lattice-gas automata *Phys. Rev. Lett.* **61** 2332–5

[2] Van Der Sman R G M 2006 Galilean invariant lattice Boltzmann scheme for natural convection on square and rectangular lattices *Phys. Rev.* E **74** 026705

[3] Jami M, Mezrhab A, Bouzidi M and Lallemand P 2007 Lattice Boltzmann method applied to the laminar natural convection in an enclosure with a heat-generating cylinder conducting body *Int. J. Thermal Sci.* **46** 38–47

[4] Zheng H W, Shu C and Chew Y T 2006 A lattice Boltzmann model for multiphase flows with large density ratio *J. Comput. Phys.* **218** 353–71

[5] Dawson S P, Chen S and Doolen G D 1993 Lattice Boltzmann computations for reacting-diffusion equations *J. Chem. Phys.* **98** 1514–23

[6] Niu X D, Yamaguchi H and Yoshikawa K 2009 Lattice Boltzmann model for simulating temperature-sensitive ferrofluids *Phys. Rev.* E **79** 046713

[7] Huang H B, Lee T S and Shu C 2007 Hybrid lattice-Boltzmann finite-difference simulation of axisymmetric swirling and rotating flows *Int. J. Numer. Methods Fluids* **53** 1707–26

[8] Sukop M C and Thorne D T 2006 *Lattice Boltzmann Modeling: An Introduction for Geoscientists and Engineers* 1st edn (Berlin: Springer)

[9] Inamuro T 2002 A lattice kinetic scheme for incompressible viscous flows with heat transfer *Phil. Trans. R. Soc.* A **360** 477–84

[10] Guo Z L, Shi B C and Zheng C G 2002 A coupled lattice BGK model for the Boussinesq equations *Int. J. Numer. Methods Fluids* **39** 325–42

[11] Parmigiani A, Huber C, Chopard B, Latt J and Bachmann O 2009 Application of the multi distribution function lattice Boltzmann approach to thermal flows *Eur. Phys. J. Special Topics* **171** 37–43

[12] Chen S, Tölke J, Geller S and Krafczyk M 2008 Lattice Boltzmann model for incompressible axisymmetric flows *Phys. Rev.* E **78** 046703

[13] Rasin I, Succi S and Miller W 2005 A multi-relaxation lattice kinetic method for passive scalar diffusion *J. Comput. Phys.* **206** 453–62

[14] Suga S 2006 Numerical schemes obtained from lattice Boltzmann equations for advection–diffusion equations *Int. J. Mod. Phys.* C **17** 1563–77

[15] Chopard B, Falcone J L and Latt J 2009 The lattice Boltzmann advection–diffusion model revisited *Eur. Phys. J. Special Topics* **171** 245–9

[16] Inamuro T, Yoshino M, Inoue H, Mizuno R and Ogino F 2002 A lattice Boltzmann method for a binary miscible fluid mixture and its application to a heat-transfer problem *J. Comput. Phys.* **179** 201–15

[17] Rothman D H and Zaleski S 1997 *Lattice-Gas Cellular Automata* (Cambridge, UK: Cambridge University Press)

[18] Huber C, Parmigiani A, Chopard B, Manga M and Bachmann O 2008 Lattice Boltzmann model for melting with natural convection *Int. J. Heat Fluid Flow* **29** 1469–80

[19] Huber C, Chopard B and Manga M 2010 A lattice Boltzmann model for coupled diffusion *J. Comput. Phys.* **229** 7956–76

[20] Guo Z L, Zheng C G and Shi B C 2002 An extrapolation method for boundary conditions in lattice Boltzmann method *Phys. Fluids* **14** 2007–10

[21] Bouzidi M, Firdaouss M and Lallemand P 2001 Momentum transfer of a Boltzmann-lattice fluid with boundaries *Phys. Fluids* **13** 3452–9
[22] Hou S L, Zou Q, Chen S Y, Doolen G and Cogley A C 1995 Simulation of cavity flow by the lattice Boltzmann method *J. Comput. Phys.* **118** 329–47
[23] He X Y, Zou Q S, Luo L S and Dembo M 1997 Analytic solutions of simple flows and analysis of nonslip boundary conditions for the lattice Boltzmann BGK model *J. Stat. Phys.* **87** 115–36
[24] Zou Q S and He X Y 1997 On pressure and velocity boundary conditions for the lattice Boltzmann BGK model *Phys. Fluids* **9** 1591–8
[25] Kao P H and Yang R J 2007 Simulating oscillatory flows in Rayleigh–Benard convection using the lattice Boltzmann method *Int. J. Heat Mass Transfer* **50** 3315–28
[26] Latt J, Chopard B, Malaspinas O, Deville M and Michler A 2008 Straight velocity boundaries in the lattice Boltzmann method *Phys. Rev.* E **77** 056703
[27] He X Y, Chen S and Doolen G D 1998 A novel thermal model for the lattice Boltzmann method in incompressible limit *J. Comput. Phys.* **146** 282–300
[28] He X Y and Luo L S 1997 Theory of the lattice Boltzmann method: from Boltzmann equation to the lattice Boltzmann equation *Phys. Rev.* E **56** 6811–7
[29] de Vahl Davis G 1983 Natural convection in a square cavity: a comparison exercise *Int. J. Numer. Methods Fluids* **3** 227–48
[30] Patterson J and Imberger J 1980 Unsteady natural convection in a rectangular cavity *J. Fluid Mech.* **100** 65–86
[31] Landau L D and Lifschitz E M 1987 *Fluid Mechanics* 2nd edn (Oxford: Pergamon)
[32] Zhou J G 2008 Axisymmetric lattice Boltzmann method *Phys. Rev.* E **78** 036701
[33] Huang H B and Lu X-Y 2009 Theoretical and numerical study of axisymmetric lattice Boltzmann models *Phys. Rev.* E **80** 016701